working paper

9714

# Interest Rate Option Pricing with Volatility Humps

by Peter Ritchken and Iyuan Chuang

FEDERAL RESERVE BANK OF CLEVELAND

Working Paper 9714

# INTEREST RATE OPTION PRICING WITH VOLATILITY HUMPS

by Peter Ritchken and Iyuan Chuang

The authors are on the faculty of the Weatherhead School of Management, Case Western Reserve University. Peter Ritchken gratefully acknowledges financial support from the Federal Reserve Bank of Cleveland.



December 1997

## Abstract

This paper develops a simple model for pricing interest rate options. Analytical solutions are developed for European claims and extremely efficient algorithms exist for the pricing of American options. The interest rate claims are priced in the Heath-Jarrow-Morton paradigm, and hence incorporate full information on the term structure. The volatility structure for forward rates is humped, and includes as a special case the exponentially dampened volatility structure used in the Generalized Vasicek model. The structure of volatilities is captured without using time varying parameters. As a result, the volatility structure is stationary. It is not possible to have all the above properties hold in a Heath Jarrow Morton model with a single state variable. It is shown that the full dynamics of the term structure can, however, be captured by a three state Markovian system. As a result, simple path reconecting lattices cannot be constructed to price American claims. Nonetheless, we provide extremely efficient lattice based algorithms for pricing claims, which rely on carrying small matrices of information at each node. Empirical support for the models developed are provided.

# 1 Introduction

This article deals with the pricing of interest rate claims when interest rates are stochastic. The methodology incorporates all current information in the yield curve. In particular, the models developed are all cast in the Heath, Jarrow and Morton (1992) paradigm (hereafter HJM). The models we propose have the following properties. First, simple analytical solutions are available for most European claims. Second, the volatility of forward rates is humped, consistent with empirical evidence. Third, the volatility structure of forward rates is a stationary function, in that it only depends on the maturity of the rate.[1] Fourth, the model includes, as a special case, the generalized Vasicek models developed by Jamshidian (1989), HJM (1992) and Hull and White (1990), as well as the continuous time Ho-Lee (1988) model. Fifth, the model permits the efficient computation of American interest rate claims. Finally, the single factor models we present readily generalize to multifactor models.

The need for simple analytical solutions for European claims cannot be understated. In particular, an important property of any derivatives model is that it not only prices discount bonds at their observable values, but it also produces theoretical prices for an array of liquid derivatives that closely match their observable values. Typically, the calibration procedure is accomplished using the discount function as well as the prices of liquid caps and swaption contracts. In the HJM paradigm, all discount bonds will be automatically priced correctly. The parameters of the volatility structure, however, need to be determined so as to closely price a set of interest rate derivative contracts. This is usually accomplished by minimizing the sum of squared residuals. With many parameters, and with a highly non linear objective function, the optimization problem is non trivial, and multiple calls to valuation routines for the individual contracts arise. If these individual routines are not efficient, then implied estimation of the parameters becomes difficult. As a result, an important criterion for successful implementation is the ease in which the model's parameters can be readily calibrated. Since our simple model can easily be calibrated, it is likely to be more successful than a more complex model which might capture more precisely the volatility structure, but at the expense of forgoing analytical solutions and hence incurring costly calibrations.

The article proceeds as follows. In the next section we review the pricing mechanism in the HJM paradigm as well as the empirical evidence regarding the volatility hump. In section 3 we develop specific models for pricing European claims. We construct a two and three state-variable model, which includes as a special case the one state generalized Vasicek model. Analytical solutions for European options are provided. In section 4 efficient algorithms for pricing American claims are pro-

[1] In particular, there are no time varying parameters in the model.

vided. The algorithms are similar in spirit to those of Li, Ritchken and Sankarasubramanian (1995). Their model involves one source of uncertainty, yet require two state variables. Here, we also have one source of uncertainty. However, up to three state variables are necessary to fully capture the dynamics of the term structure. We illustrate the convergence behavior of our algorithms. Section 5 illustrates how the analysis generalizes to two sources of uncertainty, section 6 provides some empirical support for the humped volatility model and section 7 summarizes our findings.

## 2 Pricing Mechanisms for Derivatives

Let $f(x,T)$ be the forward rate at date $x$ for the instantaneous rate beginning at date $T$. Forward rates are assumed to follow a diffusion process of the form

$$df(x,T) = \mu_f(x,T)dt + \sigma_f(x,T)dw(x) \tag{1}$$

with the forward rate function $f(0,\bullet)$ initialized to its currently observable value. Here $\mu_f(x,T)$ and $\sigma_f(x,T)$ are the drift and volatility parmeters which could depend on the level of the forward rate itself, and $dw(x)$ is the standard Wiener increment. HJM (1992) have shown that to avoid riskless arbitrage the drift term must be linked to the volatility term by:

$$\mu_f(x,T) = \sigma_f(x,T)[\lambda(x) + \sigma_p(x,T)] \tag{2}$$

where $\sigma_p(x,T) = \int_x^T \sigma_f(x,v)dv$ and $\lambda(x)$ is the market price of interest rate risk, which is independent of the maturity date $T$. Substituting equation (2) into (1) and integrating leads to

$$f(x,T) = f(0,T) + \int_0^x \sigma_f(v,T)[\sigma_p(v,T) + \lambda(v)]dv + \int_0^x \sigma_f(v,T)dw(v) \tag{3}$$

Now consider the pricing of an European claim that promises the holder a payout of $g(t)$ at date $t$. Here $g(t)$ is a cash flow fully determined by the entire term structure at that date. The arbitrage free price of this claim at date 0 is given by:

$$g(0) = E_0[g(t)]P(0,t) \tag{4}$$

where $P(0,t)$ is the price at date 0 of a bond that pays \$1 at date $T$. This expectation is computed under the *forward risk adjusted* process, which loosly speaking, is obtained by pretending $\lambda(v) = -\sigma_p(v,t)$ in equation (2). With this substitution, equation (3) can be written as:

$$f(t,T) = f(0,T) + h_1(t,T) + \int_0^t \sigma_p(v,T)dw(v) \tag{5}$$

where

$$
\begin{aligned}
h_1(t,T) &= \int_0^t g_1(v;t,T)dv \\
g_1(v;t,T) &= \sigma_f(v,T)\int_t^T \sigma_f(v,s)ds
\end{aligned}
$$

For pricing European claims it is usually easier to work under the forward risk adjusted process. In contrast, for pricing American claims, one usually proceeds by valuing under the *risk neutralized* process. In particular, as an alternative to equation (4), we have:

$$g(0) = \overline{E}_0[e^{-\int_0^t r(s)ds} g(t)] \tag{6}$$

The risk neutralized process can be viewed as a process where the market price of risk at date $v$ is taken to be 0. Under this process, equation (3) reduces to

$$f(t,T) = f(0,T) + h_2(t,T) + \int_0^t \sigma_p(v,T)dw(v) \tag{7}$$

where

$$
\begin{aligned}
h_2(t,T) &= \int_0^t g_2(v;T)dv \\
g_2(v;T) &= \sigma_f(v,T)\sigma_p(v,T)
\end{aligned}
$$

From a valuation perspective, the HJM paradigm provides a framework where, given an initial term structure, the pricing mechanism can proceed once the volatility structure of forward rates is specified. The simpliest volatility structure in the HJM paradigm is the constant volatility structure given as $\sigma_f(v,T) = \sigma$. This structure assumes all rates respond to a shock in the same way. Cursory empirical evidence suggests that volatilities of forward rates depend on their maturities. HJM (1993) and Jamshidian (1989) consider an exponentially dampened structure

$$\sigma_f(t,T) = \sigma e^{-\kappa(T-t)}.$$

This structure, referred to as the Generalized Vasicek or GV structure, implies that distant forward rates are much less volatile than near forward rates. If volatilities have this structure, then it can be shown that the entire dynamics of the term structure can be characterized by a *single* state variable, which could be the instantaneous spot rate, $r(t) = f(t,t)$, and that bond prices can be represented as

$$P(t,T) = \frac{P(0,T)}{P(0,t)} e^{-\beta(t,T)[r(t)-f(0,t)]-\frac{1}{2}\beta^2(t,T)\phi(t)} \tag{8}$$

where

$$\beta(t,T) = \frac{1}{\kappa}[1 - e^{-\kappa(T-t)}]$$

$$\phi(t) = \frac{\sigma^2}{2\kappa}[1 - e^{-2\kappa t}].$$

Ritchken and Sankarasubramanian (1995) show that if volatilities are not of this form then there is no single state variable HJM representation for the dynamics of the term structure.

There appears to be very little empirical support for an exponentially dampened forward rate volatility structure. Several researchers report a hump in the volatility structure that peaks at around the two year maturity. Heath, Jarrow Morton and Spindel (1992) provide cursory evidence of such a hump. Amin and Morton (1994) use Eurodollar futures and options and obtain negative estimates of $\kappa$ over the short end of the curve. Since negative estimates over the entire maturity spectrum are not plausible, they argue that there is a hump in the structure. Goncalves and Issler (1996) estimate the term structure of volatility using a simple GV model. Their historical analysis of forward rates also reveals a hump.[2] In addition to not providing for a volatility hump, GV models have the undesirable property that volatilities of yields are independent of their levels. As a result, interest rates can go negative. These problems have lead researchers to consider richer classes of volatility structures in which volatilities are linked directly or indirectly to the level of the term structure.

While the HJM paradigm permits the volatility structure to be quite general, unless constraints are imposed on the family of volatilities, a *finite* state representation of the term structure is not permissible. Ritchken and Sankarasubramanian (1995) characterize the set of restrictions on volatilities that permit a two state variable representation. In particular they show that if the volatility has the form

$$\sigma_f(t, T) = \sigma_r(t)k(t, T)$$

where $\sigma_r(t)$ is a function that depends on all information up to date t, and $k(t, T)$ is a deterministic function satisfying the following semi-group property:

$$\begin{aligned} k(t, T) &= k(t, u)k(u, T) \quad for \;\; t \leq u \leq T \\ k(u, u) &= 1 \end{aligned}$$

then, conditional on knowing the initial term structure, knowledge of any two points on the term structure at date $t$ is sufficient to characterize the full yield curve at that date. The class of volatility structures in this family is quite large. However, no analytical solutions have been derived for European claims. As a result, calibration issues remain, which inhibit the easy implementation of these models.

[2] Not all studies indicate the existence of a hump. For example, Bliss and Ritchken (1995) use term structure data alone and find that relative to the volatility at the short end, forward rate volatilities appear to decline with maturity.

In the next section we propose generalizing the GV model in such a way that the volatility structure is humped. By maintaining deterministic volatility structures, analytical solutions to interest rate claims is plausible. While deterministic structures do have limitations, by incorporating the volatility hump, and by yielding a pricing mechanism that permits analytical solutions to be derived for European options, efficient calibration and yields efficient pricing of American claims can be accomplished.

## 3 Option Pricing with a Volatility Hump

Assume the volatility structure is given by:

$$\sigma_f(x,T) = [a_0 + a_1(T-x)]e^{-\kappa(T-x)} + b_0 \tag{9}$$

This volatility function reduces to the GV structure when $a_1 = b_0 = 0$. Bhar and Chiarella (1995) have considered similar structures for volatilities. Indeed, they show that a *finite* state Markov representation is permissible for the term structure if the coefficient of the exponentially dampened term is a finite degree polynomial in the maturity $T - x$. Figure 1 shows a typical curve, in which the peak occurs around the two year point.

[Figure 1 Here]

For $0 \le x \le t$, the volatility structure can be expressed as:

$$\sigma_f(x,T) = d_0(t,T) + d_1(t,T)e^{-\kappa(t-x)} + d_2(t,T)[t-x]e^{-\kappa(t-x)} \tag{10}$$

where

$$\begin{aligned}
d_0(t,T) &= b_0 \\
d_1(t,T) &= [a_0 + a_1(T-t)]e^{-\kappa(T-t)} \\
d_2(t,T) &= a_1 e^{-\kappa(T-t)}
\end{aligned}$$

Substituting equation (10) into equation (5) yields:

$$f(t,T) = f(0,T) + h_1(t,T) + \sum_{i=0}^{2} d_i(t,T)W_i(t) \tag{11}$$

where

$$W_0(t) = \int_0^t dw(v) \tag{12}$$

$$W_1(t) = \int_0^t e^{-\kappa(t-v)} dw(v) \tag{13}$$

$$W_2(t) = \int_0^t (t-v) e^{-\kappa(t-v)} dw(v) \tag{14}$$

and the exact expression for $h_1(t,T)$ is provided in the appendix.

Proposition 1 *If the volatility structure is given by equation (9), and the dynamics of the forward rates are given by equation(1), then, under the FRA process, bond prices at date t are linked to prices at date 0 through three state variables, $W_0(t)$, $W_1(t)$ and $W_2(t)$ as:*

$$P(t,T) = A(t,T)e^{-R(t,T)} \tag{15}$$

*where*

$$A(t,T) = \frac{P(0,T)}{P(0,t)} e^{-H_1(t,T)}$$

$$R(t,T) = \sum_{i=0}^{2} D_i(t,T) W_i(t)$$

*and*

$$\begin{aligned} D_0(t,T) &= b_0(T-t) \\ D_1(t,T) &= \frac{1}{\kappa^2}[a_1 + a_0\kappa - (a_1\kappa(T-t) + a_0\kappa + a_1)e^{-\kappa(T-t)}] \\ D_2(t,T) &= \frac{a_1}{\kappa}[1 - e^{-\kappa(T-t)}] \end{aligned}$$

*The dynamics of the state variables, $W_1(t)$, and $W_2(t)$ are:*

$$dw_1(t) = -\kappa W_1(t)dt + dw(t) \tag{16}$$

$$dw_2(t) = [W_1(t) - \kappa W_2(t)]dt \tag{17}$$

Proof: See Appendix.

When $b_0 = 0$, $D_0(t,T) = 0$, and the number of state variables reduces to 2. Further, when $a_1 = b_0 = 0$, then, the number of state variables reduces to 1, the GV volatility structure is recovered and the bond pricing equation reduces to equation (8).

Under the FRA process, viewed from date 0, the bond price, $P(t,T)$, has a lognormal distribution. In particular, $R(t,T)$ is normal with mean 0 and variance $\gamma^2(t,T)$, where:

$$\gamma^2(t,T) = \sum_{j=0}^{2}\sum_{i=0}^{2} D_i(t,T)D_j(t,T)Cov_0(W_i(t), W_j(t)) \tag{18}$$

and

$$
\begin{aligned}
Var_0(W_0(t)) &= t \\
Var_1(W_1(t)) &= \frac{1}{2\kappa}[1 - e^{-2\kappa t}] \\
Var_2(W_2(t)) &= \frac{1}{4\kappa^3}[1 - (1 + 2\kappa t + 2\kappa^2 t^2)e^{-2\kappa t}] \\
Cov_0(W_0(t), W_1(t)) &= \frac{1}{\kappa}[1 - e^{-\kappa t}] \\
Cov_0(W_0(t), W_2(t)) &= \frac{1}{\kappa^2}[1 - (1 + \kappa t)e^{-\kappa t}] \\
Cov_0(W_1(t), W_2(t)) &= \frac{1}{4\kappa^2}[1 - (1 + 2\kappa t)e^{-2\kappa t}]
\end{aligned}
$$

We now can compute analytical solutions for a large family of European interest rate claims. Proposition 2 provides the solution to an European option on a discount bond.

**Proposition 2** *If the volatility structure is given by equation (9), then the price of a contract that provides the holder with the right to buy at date t, a bond that matures at date T, for \$X is given by:*

$$C(0) = P(0,T)N(d_1) - XP(0,t)N(d_2) \tag{19}$$

*where*

$$
\begin{aligned}
d_1 &= \frac{log(A(t,T)/X) + \gamma^2(t,T)}{\gamma(t,T)} \\
d_2 &= d_1 - \gamma(t,T)
\end{aligned}
$$

*and $\gamma^2(t,T)$ is given by equation (18).*

Proof: See Appendix.

Notice that when $a_1 = b_0 = 0$, the formula reduces to the GV option model of Jamshidian (1989).

# 4 Pricing American Options Under Humped Volatilities

The advantage of a simple deterministic volatility structure as in equation (9), is that it permits the development of analytical solutions for many European claims including caps, floors, and swaptions. The resulting expressions have the same form as their simple GV counterparts, except the volatility expression ($\gamma(t,T)$) takes on a more complex form. Analytical solutions for such claims are useful since they reduce the complexity of the calibration process. Once the parameters are estimated, then lattice based algorithms can be used to price a variety of American claims and some interest rate exotics. In this section we describe such algorithms.

The valuation procedure takes place using the risk neutralized measure. Under this measure the term structure at date $t$ is given by:

$$f(t,T) = f(0,T) + h_2(t,T) + \int_0^t \sigma_p(v,T)dw(v) \tag{20}$$

and the bond pricing equation is:

$$P(t,T) = A(t,T)e^{-R(t,T)} \tag{21}$$

where

$$\begin{aligned} A(t,T) &= \frac{P(0,T)}{P(0,t)}e^{-H_2(t,T)} \\ R(t,T) &= \sum_{i=0}^{2} D_i(t,T)W_i(t) \\ H_2(t,T) &= \int_t^T h_2(t,x)dx. \end{aligned}$$

Assume the time interval $[0,t]$ is partitioned into $n$ equal subintervals of width $h$. A simple binomial lattice is used to approximate the standard Wiener process. Let $W^a_{0,i}$ approximate the process at time $ih$ for $i = 0, 1, 2, ...., n$, with $W^a_{0,0} = 0$. Given $W^a_{0,i}$, the next permissible values are $W^a_{0,i} + \sqrt{h}$ and $W^a_{0,i} - \sqrt{h}$, which both occur with probability 0.5. For pricing purposes, the term structure can be recovered at each node of the lattice if the exact values of the three state varibales are given. Let $(W^a_1, W^a_2)$ be the values of the two state variables at a particular node, where the first state variable has value $W^a_0$. The number of different values for the state variables $W^a_1$ and $W^a_2$ at this node equals the number of different paths that can be traversed from the originating node to this point. Rather than keep track of all these values, we follow the basic idea of Li, Ritchken and Sakarasubramanian (1996) and only keep track of the maximum and minimum values that each of the two state variables can attain at each node. The range between the maximum and minimum values is then partitioned into $k_1$ and $k_2$ pieces respectively. Option prices are then kept track of at the resulting $k_1 \times k_2$ points. Thus at each node in the lattice, a matrix of option values needs to be established.

Let $C(i,j)$ be the $(i,j)^{th}$ entry for a price that is to be computed at the node $W^a_0$ and assume $W^a_1 = y$ and $W^a_2 = z$. Assume the date is $mh$ say, for some integer $m \leq (n-1)$. Given these two state variables, their successor values at date $(m+1)h$ can be computed using approximations to equations (16) and (17). In particular, the two successor nodes are $(a + \sqrt{h})$ and $(a - \sqrt{h})$ both of which occur with probability 0.5. The values of the two state variables, obtained using equations (16) and (17), at these two nodes, are $(y-(\kappa yh)+\sqrt{h}, z+(y-\kappa z)h)$ and $(y-(\kappa yh)-\sqrt{h}, z+(y-\kappa z)h)$ respectively. Option prices at the succcessor nodes, for these particular state variables, may not be available. However, option prices at "surrounding" states will be available, and interpolation procedures can be used to establish an option price. The average of the option prices computed in both the up state and down state can then be computed, and the resulting value discounted by the current one period bond price, provides the value of the option unexercised at the current location. The maximum of this value and the exercised value of the claim provides the numerical value for $C(i,j)$.

When computing option prices using backward recursion, various interpolation techniques can be used to establish the values of the claim in both successor states. Li, Ritchken and Sankarasubramanian (1995), show that relatively coarse partitions of the range of the state variable at each node, combined with simple linear interpolation methods produce satisfactory results for their problem.[3]

We first report on the performance of an algorithm for the volatility structure in equation (9) with $a_1 = 0$. In this case there are only two state variables. Since analytical solutions are available for European options on bonds, we use these contracts to illustrate the convergence behavior for the contract as the number of time partitions, $n$, and as the number of space partitions, $k_1$, increase. Figure 2 reports the results for the one year at-the-money option, when a simple linear interpolation method is used.

[Figure 2 Here]

Notice, that for all time partitions, as $k_1$ is increased the convergence rate improves. Notice too, that reasonably accurate results for option prices are obtained for 50 time partitions and about 5 space partitions.[4]

Table 1 compares the convergence rate of prices for various space partitions using a linear interpolation scheme, to the case where only 3 points are used to approximate the state variable at each node, but a quadratic approximation is invoked. As can be seen, the quadratic approximation works very effectively, producing accurate results even for a small number of time partitions.

[Table 1 Here]

[3]For example, they show that partitions of size 10 to 20 produce prices of options on bonds that are practically indistinguishable.

[4]Similar results hold over the full range of parametrs for the volatility structure.

Figure 3 shows the convergence of option prices to the analytical solution for the general volatility structure with $a_1 \neq 0$. In Figure 3 the partition sizes ($k_1$ and $k_2$) for the two state variables $W_1(t)$ and $W_2(t)$ are taken to be equal.

[Figure 3 Here]

Table 2 shows the effects of using a quadratic approximation scheme rather than linear interpolation. Using just three points for each state variable at each node appears to suffice. These results are quite robust to the parameter values for the volatility structure.

[Table 2 Here]

# 5 Multifactor Models

The above analysis readily generalizes to multifactor models. In this section we consider a specific two factor model which has the property that the factors are correlated. In particular assuming the following dynamics for forward rates:

$$df(t,T) = \mu_f(t,T)dt + \sigma_{f_1}(t,T)dw_1(t) + \sigma_{f_2}(t,T)dw_2(t) \tag{22}$$

where

$$\begin{aligned} \sigma_{f_1}(t,T) &= a_0 e^{-\kappa(T-t)} \\ \sigma_{f_2}(t,T) &= b_0 \\ E[dw_1 dw_2] &= \rho dt \end{aligned}$$

This model differs from simple two factor GV model, in that the two factors are correlated. Transforming this model, we obtain:

$$df(t,T) = \mu_f(t,T)dt + (a_0 e^{-\kappa(T-t)} + \rho b_0)d\xi_1(t) + (\sqrt{1-\rho^2})b_0 d\xi_2(t) \tag{23}$$

where $d\xi_1$ and $d\xi_2$ are standard independent Wiener increments with $E[d\xi_1 d\xi_2] = 0$. Moreover, under the forward risk adjusted process,

$$\mu_f(x,T) = \sum_{i=1}^{2} \int_0^t [\sigma_{f_i}(x,T) \int_x^T \sigma_{f_i}(x,s)ds]$$

Now, from equation (23)

$$f(t,T) = f(0,T) + h_1(t,T) + d(t,T)Z(t) + \rho b_0 \xi_1(t) + \sqrt{1-\rho^2} b_0 \xi_2(t)$$

where

$$
\begin{aligned}
d(t,T) &= a_0 e^{-\kappa(x-t)} dx \\
Z(t) &= \int_t^T e^{-\kappa(t-x)} d\xi_1(x) \\
h_1(t,T) &= \int_t^T \sum_{i=1}^{2} \int_0^t [\mu_f(x,T) dx
\end{aligned}
$$

Further, the bond price can be computed as

$$
P(t,T) = A(t,T) e^{-R(t,T)}
$$

where

$$
\begin{aligned}
A(t,T) &= \frac{P(0,T)}{P(0,t)} e^{-H_1(t,T)} \\
R(t,T) &= D(t,T)Z(t) + \rho b_0(T-t)\xi_1(t) + (\sqrt{1-\rho^2}) b_0(T-t)\xi_2(t) \\
H_1(t,T) &= \int_t^T h_1(t,x) dx \\
D(t,T) &= \int_t^T d(t,x) dx
\end{aligned}
$$

This two factor model is characterized by three state variables. Straightforward lattice procedures as outlined above can then be used to proxy the dynamics of the term structure. Analytical solution for European options on discount bonds are permissible. Similar to Proposition 2, we can obtain the price of a contract that provides the holder with the right to buy at date t, a bond that matures at date $T$, for \$$X$ as:

$$
C(0) = P(0,T)N(d_1) - XP(0,t)N(d_2) \tag{24}
$$

where

$$
\begin{aligned}
d_1 &= \frac{log(A(t,T)/X) + \gamma^2(t,T)}{\gamma(t,T)} \\
d_2 &= d_1 - \gamma(t,T) \\
\gamma^2(t,T) &= Var(R(t,T))
\end{aligned}
$$

## 6 Empirical Tests

In this section we provide some preliminary empirical tests on the GGV model. Our goal is to establish if there is support for the one factor GGV model and to establish whether the model can reduce out of sample biases that exist in applying the simple GV model.

We obtained a set of daily caplet data, and zero curves from Bears Stern. The data consists of prices of at-the-money caplets with maturities ranging from 1 year to 9 years in increments of 1 year. Each caplet is on a 3 month LIBOR rate. The prices are reported in Black volatility form. To translate these numbers into prices we require the discount rates for the appropriate maturities. The discount function for each day, computed using the par swap rate curve was also supplied. 10 weeks of data were provided.

In our analysis, we assume all the parameters remain constant over a week. Then we use all $9 \times 5 = 45$ option prices, to infer out the set of estimates that minimize the sum of squared error.[5] We repeat this analysis, separately for each of the 10 successive weeks. Table 3 reports the estimates of the parameters for each of the 10 optimizations for the GV and the GGV models.

[Table 3 Here]

For the GV model, the volatility and mean reversion estimates are fairly stable over the 10 weeks. For the GGV model, in addition to the estimates of the volatility parameters, we also report the forward rate maturity with the maximum volatility. This maturity is consistently close to 1.3 years, and the magnitude of the volatility there is surprisingly stable at a value near 0.015. In all 10 runs of the GGV model, the null hypothesis that the parameter values $a_1 = b_0 = 0$ is rejected at the 5% level of significance. That is, the inclusion of the volatility hump, beyond the usual GV exponentially dampened structure, adds significantly to the model.

Table 4 summarizes the in-sample residuals for the GV and GGV models. In each of the 10 weekly estimations for both models, 5 residuals are available for each maturity. This gives a total of 50 residuals. For each maturity, the number of positive and negative residuals are indicated, as well as their average and standard deviation.

[Table 4 Here]

The table immediately reveals the large biases in the GV model. All the residuals in the first year are negative, while all the residuals in years $2-4$ are positive. The large bias continues over all maturities. Figure 4$a$ illustrates the biases for a typical week. Here, the 9 residuals for each of the 5 days in the week are plotted. As can be seen, the simple exponentially dampened structure for volatilities is not flexible enough to permit pricing to proceed without introducing a large maturity bias.

[5] We minimized the sum of squared error of the pricing residuals, in dollars, and in implied volatility units. In both cases, the set of results were almost identical. As a result, we use the first objective, but report all our residuals in Black volatility form.

[Figure 4 Here]

Table 4 also reports the results for the GGV model. Relative to the GV model, a significant amount of the bias is removed. Figure 4*b* illustrates the pattern of residuals for all 5 days of a typical week.

The in sample analysis does indicate that a GV model is not capable of fitting a volatility structure that has a hump. Table 4 presents a similar analysis of residuals, this time conducted on out-of-sample data. The estimates of the volatility parameters, derived using the data in a given week, are then used to estimate the option prices for each day of the next week. That is, the volatility parameters are only updated at the end of a week, using full information on the entire week. The model is then not recalibrated until the end of the next week. As a result, for the week, we obtain $9 \times 5 = 45$ out of sample residuals for each maturity. Table 5 reports the number of positive and negative residuals as well as their means and variances for each maturity caplet.

[Table 5 Here]

The results are consistent with the results from the in-sample-residuals. In particular, much of the bias in the GV model is eliminated by the GGV model. The last row of this table reports the number of times (out of 45) that the absolute value of each GGV residual is smaller than the absolute value of the GV residual. The superior performance of the GGV model, especially over the the first 5 maturities is evident. Figure 6 provides a plot of the difference in the absolute values of the residuals. The figure confirms the fact that the GGV dominates the GV model, in that the out of sample residuals produced by GGV are generally much smaller than GV.

[Figure 6 Here]

The above results provide significant evidence that the GGV can explain prices of caplets beyond what is possible with a GV model. The final table attempts to establish whether the forecasted GGV prices of caplets are within typical bid ask spreads and whether the forecasts deteriorate over time. For each out-of-sample day, we report the distribution of the $9 \times 9 = 81$ out of sample residuals. For example, consider the one year maturity caplet. Of the 81 forcasts made for the Monday prices, 68 were within 0.25 vols of the actual price, 11 was within 0.5 vols and 2 were larger. The performance of the forecasts did deteriorate somewhat over the next 4 days. However, even if one did not recalibrate the model for 1 week, 71 out of the 81 residuals were within 0.5 vols of the actual prices. Since a typical bid ask spread of a caplet is often between 0.25 and 0.5 vols, residuals of this magnitude are respectable. The results hold true when broken down by caplet maturity.

[Table 6 Here]

Our preliminary empirical results indicate that a significant portion of the bias in the GV model can be explained by a more flexible handling of the volatility structure. Certainly, the preliminary results do indicate that the naturity structure of at-the-money caplets can be reasonably well approximated by the GGV model.

## 7 Conclusion

This paper develops a simple model for pricing interest rate options. Analytical solutions are available for European claims and extremely efficient algorithms exist for the pricing of American options. The interest rate claims are priced in the Heath-Jarrow-Morton paradigm, and hence incorporate full information on the term structure. The volatility structure for forward rates is humped, and includes as a special case the Generalized Vasicek model. The structure of volatilities is captured without using time varying parameters. As a result, the volatility structure is stationary. It is not possible to have a volatility structure with the above properties and at the same time capture the term structure dynamics by a single state variable. It is shown that the full dynamics of the term structure can, however, be captured by a three state Markovian system. As a result, simple path reconecting lattices cannot be constructed to price American claims. Nonetheless, we provide extremely efficient lattice based algorithms for pricing claims, which rely on carrying small matrices of information at each node.

Our preliminary empirical analysis provided strong support for the single factor GGV model in favor over the GV model. Moreover, the GGV model produces somewhat stable parameter estimates, and was capable of producing out of sample prices that were consistently within reasonable bid ask spreads. The results indicate that a more thorough empirical study is waranted, where a larger data set is used covering a wider family of contracts.

It also remains for future work to extend these models to handle a larger class of forward rate volatility structures. As long as the volatility structure is a sum of weighted exponential functions multiplied by maturity dependent polynomials, then a finite state variable representation is possible. When the volatility structure of forward rates belongs to the Ritchken-Sankarasubramanian class, then the analysis becomes more difficult. Extensions of our lattice procedure to handle humped volatility structures within the extended Ritchken Sankarasubramanian class will be of substantial interest.

## Appendix

*Proof of Proposition 1*

By definition of $P(t,T)$ and equation (11), we can write:

$$
\begin{aligned}
P(t,T) &= e^{-\int_t^T f(t,x)dx} \\
&= \frac{P(0,T)}{P(0,t)} e^{-\int_t^T h_1(t,x)dx - \sum_{i=0}^{2} \int_t^T d_i(t,x)dx W_i(t)} \\
&= A(t,T) e^{-R(t,T)}
\end{aligned}
$$

where

$$
\begin{aligned}
A(t,T) &= \frac{P(0,T)}{P(0,t)} e^{-H_1(t,T)} \\
R(t,T) &= \sum_{i=0}^{2} \int_t^T d_i(t,x)dx W_i(t) \\
&= \sum_{i=0}^{2} D_i(t,T) W_i(t)
\end{aligned}
$$

and

$$
\begin{aligned}
D_0(t,T) = \int_t^T d_0(t,x)dx &= b_0(T-t) \\
D_1(t,T) = \int_t^T d_1(t,x)dx &= \frac{1}{\kappa^2}[a_1 + a_0\kappa - (a_1\kappa(T-t) + a_0\kappa + a_1)e^{-\kappa(T-t)}] \\
D_2(t,T) = \int_t^T d_2(t,x)dx &= \frac{a_1}{\kappa}[1 - e^{-\kappa(T-t)}]
\end{aligned}
$$

$H_1(t,T) = \int_t^T h_1(t,x)dx$ computing this integral yields

$$
\begin{aligned}
H_1(t,T) &= b_0^2 t T^2/2 + b_0 T(-2a_1 + 2a_1 e^{\kappa t} - a_0\kappa + a_0 e^{\kappa t}\kappa - a_1\kappa t \\
&-b_0 e^{\kappa t}\kappa^3 t^2)/(e^{\kappa t}\kappa^3) \\
&-(5a_1^2 - 5a_1^2 e^{2\kappa t} + 6a_0 a_1 \kappa - 6a_0 a_1 e^{2\kappa t}\kappa + 2a_0^2\kappa^2 - 2a_0^2 e^{2\kappa t}\kappa^2 \\
&+6a_1^2\kappa t + 4a_0 a_1 \kappa^2 t - 16 b_0 a_1 e^{\kappa t}\kappa^2 t + 16 b_0 a_1 e^{2\kappa t}\kappa^2 t \\
&-8a_0 b_0 e^{\kappa t}\kappa^3 t + 8a_0 b_0 e^{2\kappa t}\kappa^3 t + 2a_1^2\kappa^2 t^2 - 8b_0 a_1 e^{\kappa t}\kappa^3 t^2 \\
&-4b_0^2 e^{2\kappa t}\kappa^5 t^3)/(8e^{2\kappa t}\kappa^5) \\
&+(-5a_1^2 + 5a_1^2 e^{2\kappa t} - 6a_0 a_1 \kappa + 6a_0 a_1 e^{2\kappa t}\kappa - 2a_0^2\kappa^2 + 2a_0^2 e^{2\kappa t}\kappa^2 \\
&-6a_1^2 e^{2\kappa t}\kappa t - 4a_0 a_1 e^{2\kappa t}\kappa^2 t + 2a_1^2 e^{2\kappa t}\kappa^2 t^2 - 6a_1^2\kappa T + 6a_1^2 e^{2\kappa t}\kappa T
\end{aligned}
$$

$$
\begin{aligned}
&-4a_0a_1\kappa^2T + 4a_0a_1e^{2\kappa t}\kappa^2T - 4a_1^2e^{2\kappa t}\kappa^2tT - 2a_1^2\kappa^2T^2 \\
&+2a_1^2e^{2\kappa t}\kappa^2T^2)/(8e^{2\kappa T}\kappa^5) \\
&+(5a_1^2 - 5a_1^2e^{2\kappa t} + 6a_0a_1\kappa - 6a_0a_1e^{2\kappa t}\kappa + 2a_0^2\kappa^2 - 2a_0^2e^{2\kappa t}\kappa^2 \\
&+3a_1^2\kappa t + 3a_1^2e^{2\kappa t}\kappa t + 2a_0a_1\kappa^2t - 8b_0a_1e^{\kappa t}\kappa^2t + 2a_0a_1e^{2\kappa t}\kappa^2t \\
&+8b_0a_1e^{2\kappa t}\kappa^2t - 4a_0b_0e^{\kappa t}\kappa^3t + 4a_0b_0e^{2\kappa t}\kappa^3t - 4b_0a_1e^{2\kappa t}\kappa^3t^2 \\
&+3a_1^2\kappa T - 3a_1^2e^{2\kappa t}\kappa T + 2a_0a_1\kappa^2T + 8b_0a_1e^{\kappa t}\kappa^2T - 2a_0a_1e^{2\kappa t}\kappa^2T \\
&-8b_0a_1e^{2\kappa t}\kappa^2T + 4a_0b_0e^{\kappa t}\kappa^3T - 4a_0b_0e^{2\kappa t}\kappa^3T + 2a_1^2\kappa^2tT \\
&-4b_0a_1e^{\kappa t}\kappa^3tT + 8b_0a_1e^{2\kappa t}\kappa^3tT + 4b_0a_1e^{\kappa t}\kappa^3T^2 - 4b_0a_1e^{2\kappa t}\kappa^3T^2) \\
&/(4e^{\kappa(t+T)}\kappa^5)
\end{aligned}
$$

*Proof of Proposition 2*

By definition of call option which expires at date $t$:

$$
\begin{aligned}
C(t) &= Max[P(t,T) - X, 0] \\
&= Max[A(t,T)e^{-R(t,T)} - X, 0]
\end{aligned}
$$

The expected payoff under the FRA measure at date $t$ is given by:

$$E_0[C(t)] = A(t,T)e^{\gamma^2(t,T)/2}N(d_1) - XN(d_2)$$

where

$$
\begin{aligned}
d_1 &= \frac{log(A(t,T)/X) + \gamma^2(t,T)}{\gamma(t,T)} \\
d_2 &= d_1 - \gamma(t,T)
\end{aligned}
$$

and $\gamma^2(t,T) = Var(R(t,T))$. From equation (4), we can write:

$$
\begin{aligned}
C(0) &= P(0,t)E_0[C(t)] \\
&= P(0,t)A(t,T)e^{\gamma^2(t,T)/2}N(d_1) - P(0,t)XN(d_2) \\
&= P(0,T)e^{-H_1(t,T)+\gamma^2(t,T)/2}N(d_1) - P(0,t)XN(d_2) \\
&= P(0,T)N(d_1) - P(0,t)XN(d_2)
\end{aligned}
$$

Note that $H_1(t,T) = \gamma^2(t,T)/2$.

## References


Amin, K., and A. Morton (1994),"Implied Volatility Functions in Arbitrage-Free Term Structure Models," *Journal of Financial Economics*, 35, 141-180.

Bhar, R., and C. Chiarella (1995),"Transformation of Heath-Jarrow-Morton Models to Markovian Systems," *Working Paper*, School of Finance and Economics, University of Technology, Sydney.

Bliss, R., and P. Ritchken (1996),"Empirical Tests of Two State-Variable HJM Models," *Forthcoming Journal of Money, Credit and Banking.*

Caverhill, A. (1994),"When Is the Short Rate Markovian?" *Mathematical Finance*, 4, 305-312.

Goncalves, and Issler (1996),"Estimating the Term Structure of Volatility and Fixed-income Derivative Pricing," *Journal of Fixed Income*, June, 32-39.

Heath, D., R. Jarrow, and A. Morton (1992),"Bond Pricing and the Term Structure of Interest Rates: A New Methodology for Contingent Claims Valuation," *Econometrica*, 60, 77-105.

Heath, D., R. Jarrow, A. Morton, and M. Spindel (1992),"Easier Done Than Said," *Risk*, 5, 77-80.

Ho, T., and S. Lee (1986),"Term Structure Movements and Pricing Interest Rate Contingent Claims," *Journal of Finance*, 41, 1011-1029.

Hull, J., and A. White (1990),"Pricing Interest Rate Derivative Securities," *Review of Financial Studies*, 3, 573-592.

Jamshidian, F. (1989),"An Exact Bond Option Formula," *Journal Finance*, 44, 205-209.

Li, A., P. Ritchken, and L. Sankarasubramanian (1995),"Lattice Models for Pricing American Interest Rate Claims," *Journal of Finance*, 50, 719-737.

Ritchken, P., and L. Sankarasubramanian (1995) ,"Volatility Structures of Forward Rates and the Dynamics of the Term Structure," *Mathematical Finance*, 5, 55-72.

**Figure 1**
**Illustration of Volatility Hump***

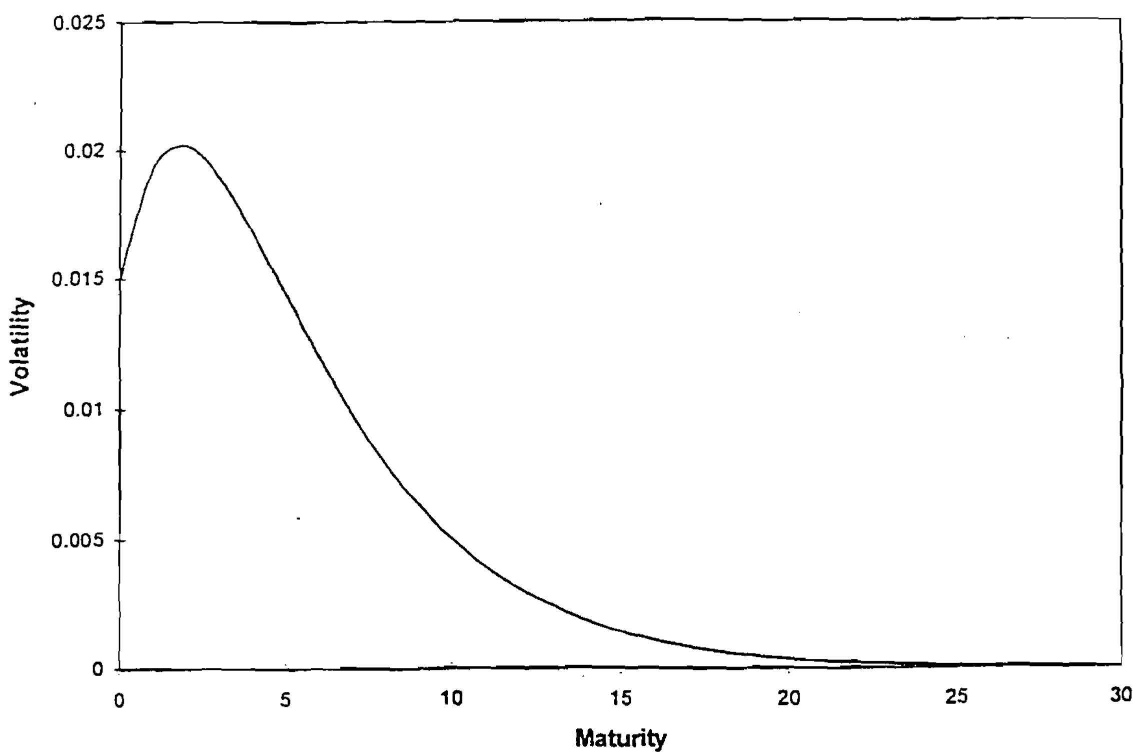


*Figure 1 shows a typical volatility structure that can be established using equation (9). In this figure $b_0 = 0$ so the volatility for long term forward rates eventually decays to zero.

**Figure 2**
**Convergence of Option Prices on The Lattice***

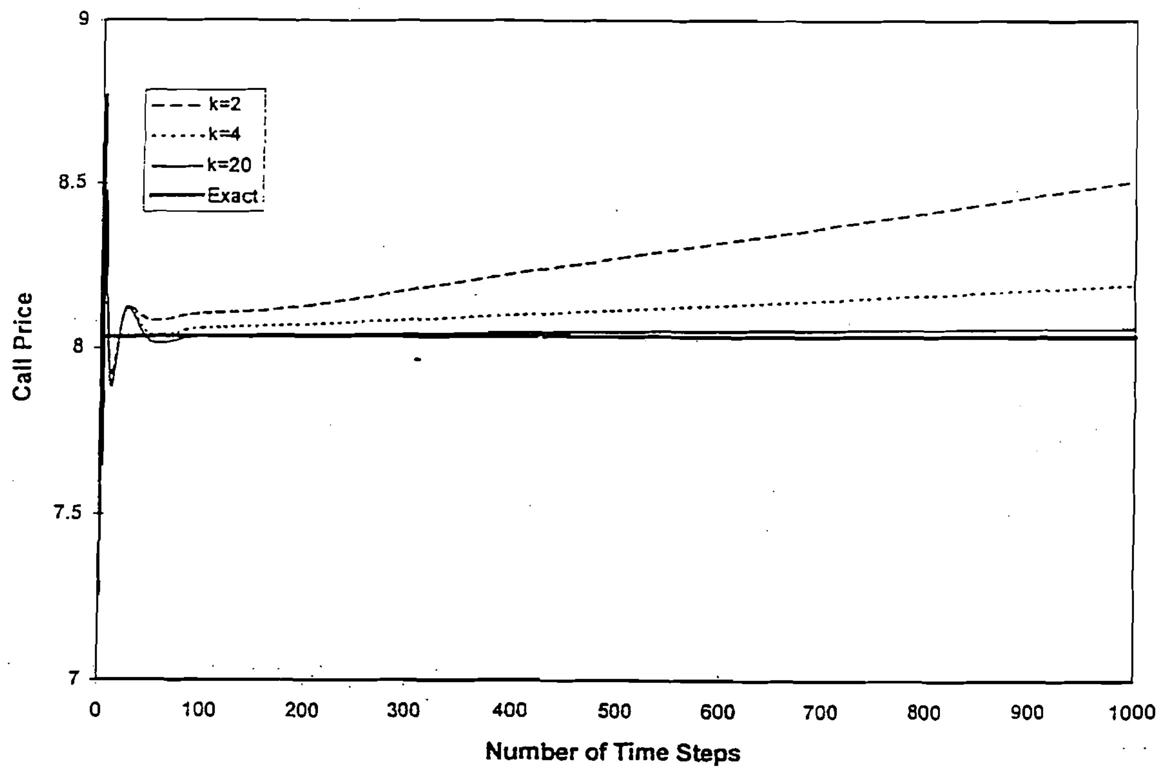


*The volatility structure for this figure is detailed in Table 1. There are two state variables for this volatility structure, so at each node in the lattice, there is a vector of prices. The size of the vector is k. The figure shows the convergence rate of prices for three different k values. The top dashed line corresponds to the case where k = 2. The middle dashed line corresponds to the case where k = 4, and the almost flat solid line corresponds to the case where k = 20. The example illustrates that accurate prices can be obtained when k is reasonably small. The option is a six month European call option on a two year bond. The exact specifications of the contract are discussed in Table 1.

**Figure 3**
**Convergence of Option Prices on The Lattice***

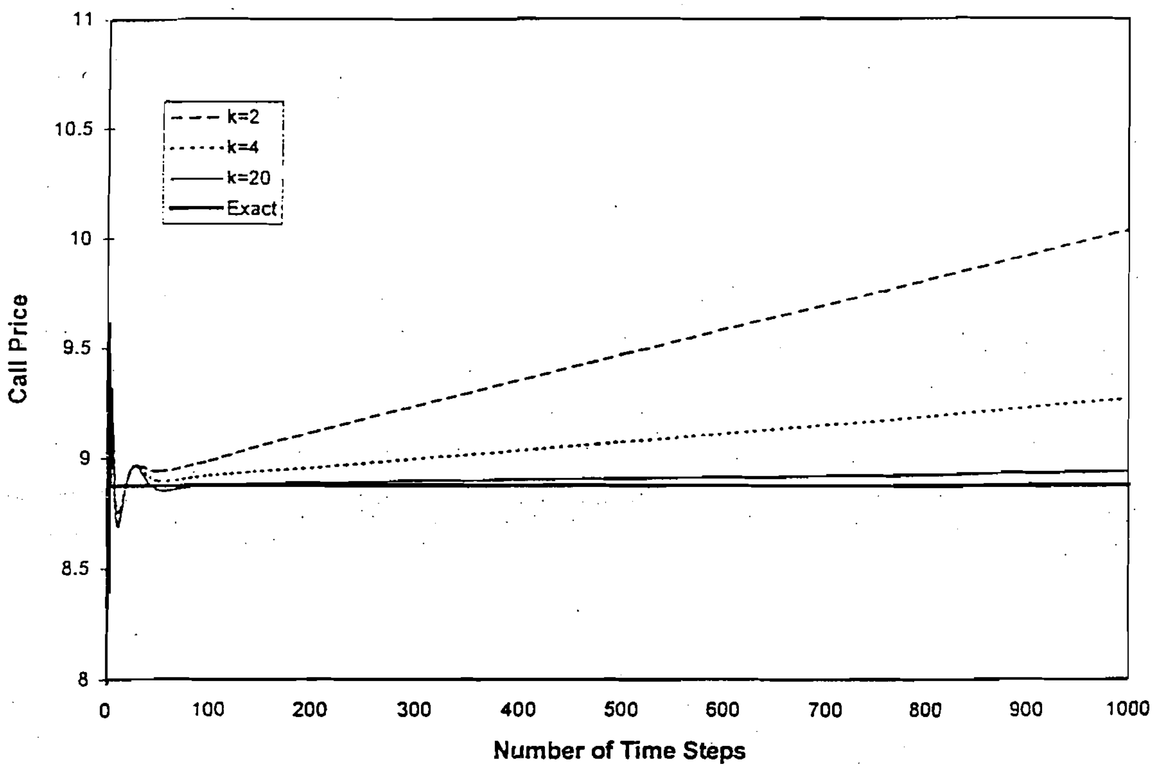


*The volatility structure for this figure is detailed in Table 2. There are three state variables for this volatility structure, so at each node in the lattice, there is a matrix of prices. The size of the matrix is $k \times k$. The figure shows the convergence rate of prices for three different k values. The top dashed line corresponds to the case where $k = 2$. The middle dashed line corresponds to the case where $k = 4$, and the almost flat solid line corresponds to the case where $k = 20$. The example illustrates that accurate prices can be obtained when k is reasonably small. The option is a six month European call option on a two year bond. The exact specifications of the contract are discussed in Table 2.

**Figure 4a**
**Plot of Daily Residuals for a Given Week (GV Model)**
**(In Sample) ***

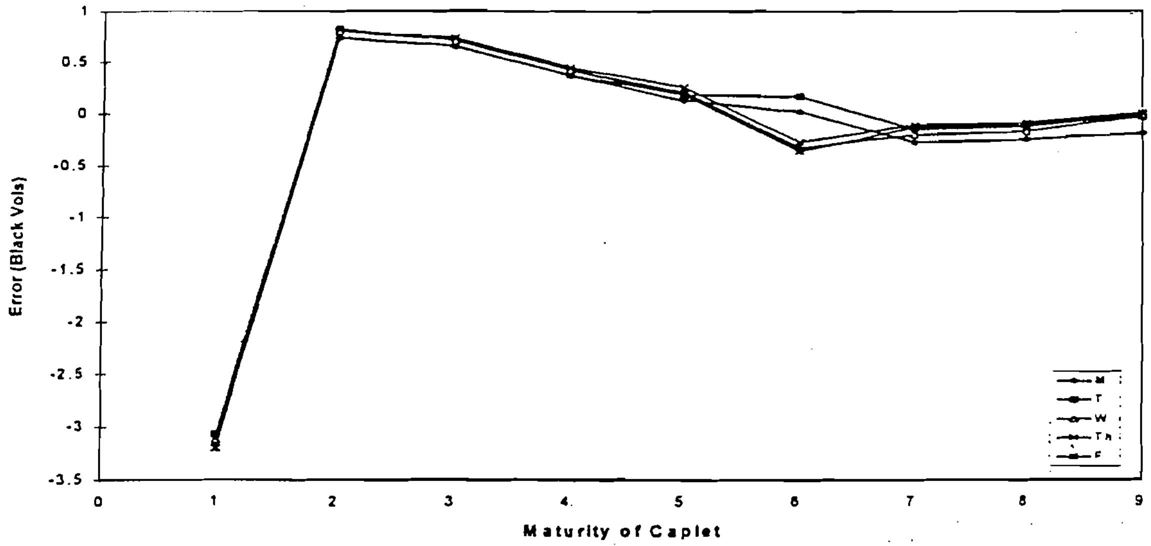


**Figure 4b**
**Plot of Daily Residuals for a Given Week (GGV Model)**
**(In Sample) ***

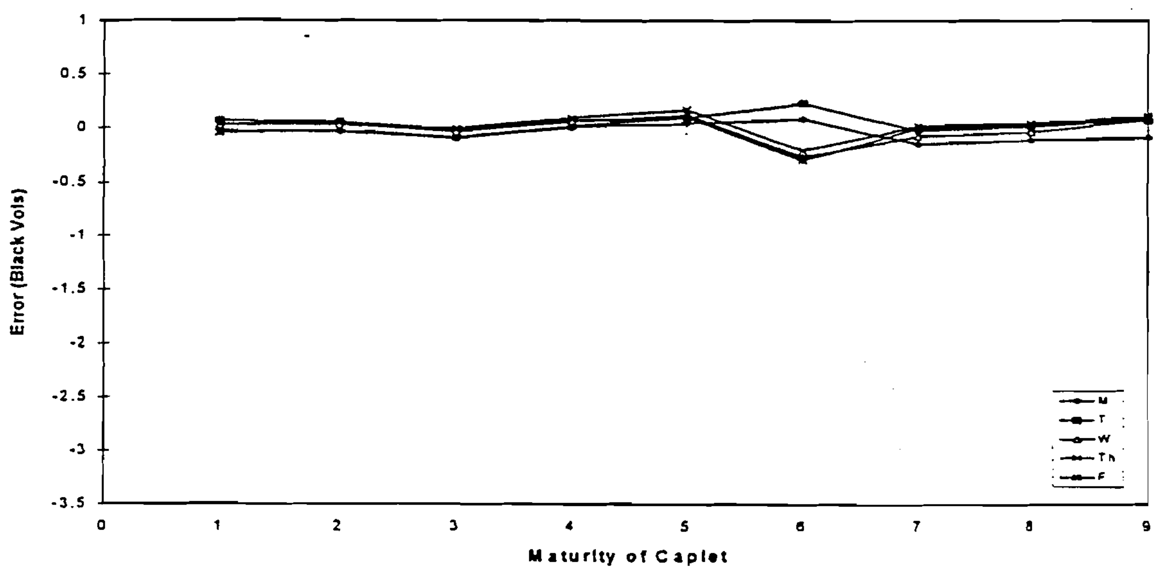


* This figure shows the residual (in Black vol form) for each caplet maturity for each day in a typical week. Figure 4a Shows the residuals for the GV model while figure 4b Shows the residuals for the GGV model.

Figure 5a
Plot of Daily Residuals for a Given Week (GV Model)
(Out of Sample) *

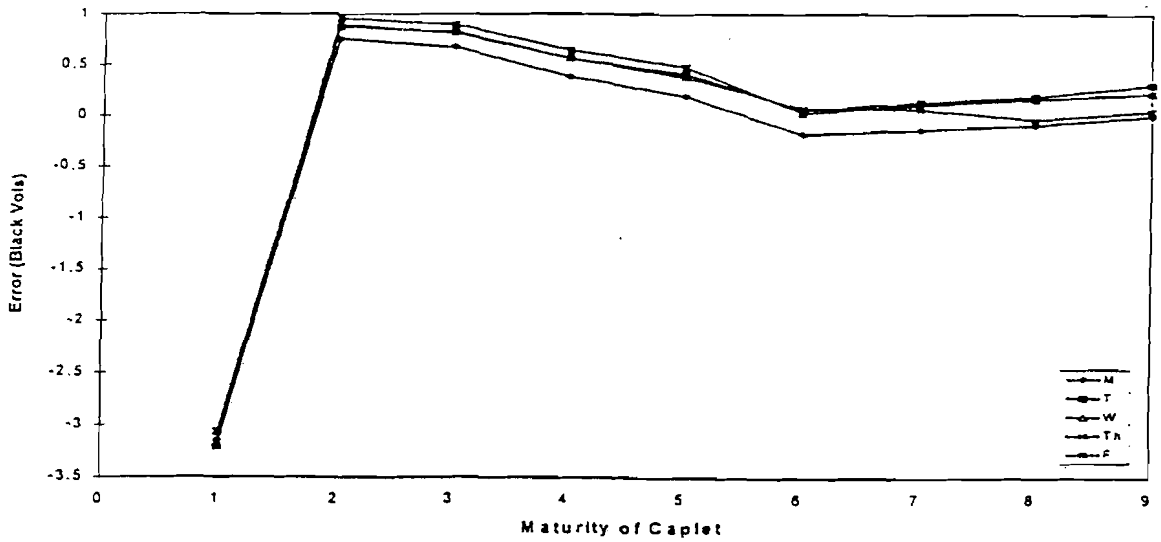


Figure 5b
Plot of Daily Residuals for a Given Week (GGV Model)
(Out of Sample) *

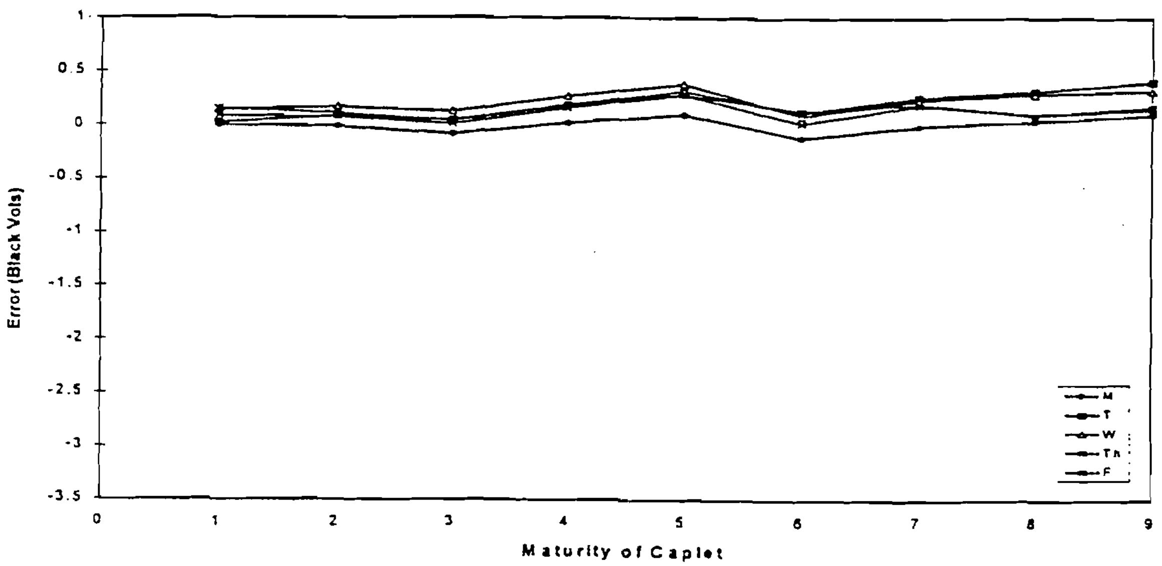


* This figure shows the residual (in Black vol form) for each caplet maturity for each day in a typical week. Figure 5a Shows the residuals for the GV model while figure 5b Shows the residuals for the GGV model.

Figure 6
Plot of Difference in Absolute Errors*

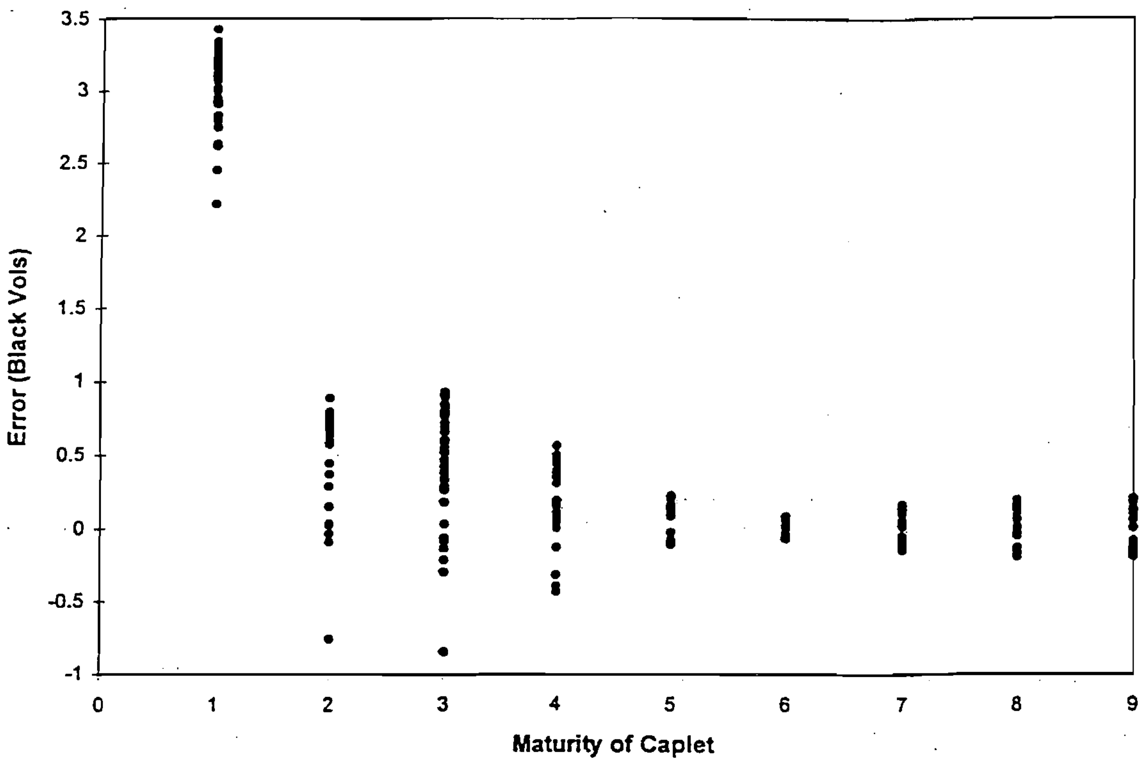


* Figure 6 shows the difference in the absolute values of the GV and GGV residuals. A positive number indicate that the GV model had a larger absolute residual.

**Tablel**
**Convergence Rate of Options With**
**Linear and Quadratic Interpolations***

| | Linear | | | | | | Quadratic |
|---|---|---|---|---|---|---|---|
| N | k=2 | k=3 | k=4 | k=10 | k=20 | k=50 | k=3 |
| 2 | 7.256 | 7.256 | 7.256 | 7.256 | 7.256 | 7.256 | 7.256 |
| 3 | 8.768 | 8.768 | 8.768 | 8.768 | 8.768 | 8.768 | 8.768 |
| 4 | 7.664 | 7.651 | 7.649 | 7.647 | 7.647 | 7.647 | 7.649 |
| 5 | 8.470 | 8.470 | 8.470 | 8.470 | 8.470 | 8.470 | 8.470 |
| 10 | 7.932 | 7.908 | 7.897 | 7.890 | 7.889 | 7.889 | 7.892 |
| 25 | 8.118 | 8.118 | 8.118 | 8.118 | 8.118 | 8.118 | 8.118 |
| 50 | 8.081 | 8.046 | 8.038 | 8.022 | 8.016 | 8.014 | 8.014 |
| 100 | 8.101 | 8.063 | 8.057 | 8.038 | 8.032 | 8.028 | 8.026 |
| 200 | 8.126 | 8.078 | 8.070 | 8.046 | 8.04 | 8.035 | 8.032 |
| 500 | 8.272 | 8.153 | 8.113 | 8.061 | 8.047 | 8.039 | 8.034 |
| 1000 | 8.506 | 8.270 | 8.191 | 8.086 | 8.059 | 8.043 | 8.034 |
| Exact | 8.033 | 8.033 | 8.033 | 8.033 | 8.033 | 8.033 | 8.033 |

*Table 1 shows the convergence rate of a call option as the number of time partitions, n, increases. The maturity of the option is 6 months. The underlying bond is a two year bond. The strike price is set equal to the current forward price, for delivery in 6 months. The table shows the convergence rate for various values of k, when linear interpolation procedures are used, and for a quadratic interpolation scheme. The initial term structure is given by:

$$f(0,t) = 0.07 - 0.02e^{-0.18t}.$$

The case parameters for the volatility structure are:

$$\kappa = 0.1,\ a_0 = 0.02,\ a_1 = 0,\ b_0 = 0.003.$$

In this case there are two state variables in the model.

Table2
Convergence Rate of Options With
Linear and Quadratic Interpolations*

| | | | Linear | | | | Quadratic |
|---|---|---|---|---|---|---|---|
| N | k=2 | k=3 | k=4 | k=10 | k=20 | k=50 | k=3 |
| 2 | 7.925 | 7.925 | 7.925 | 7.925 | 7.925 | 7.925 | 7.925 |
| 3 | 9.611 | 9.611 | 9.611 | 9.611 | 9.611 | 9.611 | 9.611 |
| 4 | 8.432 | 8.4 | 8.396 | 8.396 | 8.396 | 8.396 | 8.395 |
| 5 | 9.314 | 9.314 | 9.314 | 9.314 | 9.314 | 9.314 | 9.314 |
| 10 | 8.761 | 8.73 | 8.713 | 8.695 | 8.695 | 8.695 | 8.698 |
| 25 | 8.963 | 8.962 | 8.962 | 8.962 | 8.962 | 8.962 | 8.962 |
| 50 | 8.941 | 8.911 | 8.897 | 8.867 | 8.855 | 8.85 | 8.852 |
| 100 | 8.987 | 8.94 | 8.921 | 8.89 | 8.878 | 8.868 | 8.868 |
| 200 | 9.115 | 8.993 | 8.957 | 8.905 | 8.89 | 8.88 | 8.874 |
| 500 | 9.466 | 9.171 | 9.073 | 8.942 | 8.907 | 8.888 | 8.877 |
| 1000 | 10.031 | 9.459 | 9.266 | 9.007 | 8.938 | 8.9 | 8.877 |
| Exact | 8.876 | 8.876 | 8.876 | 8.876 | 8.876 | 8.876 | 8.876 |

*Table 2 shows the convergence rate of a call option as the number of time partitions, n, increases. The maturity of the option is 6 months. The underlying bond is a two year bond. The strike price is set equal to the current forward price, for delivery in 6 months. The table shows the convergence rate for various values of k, when linear interpolation procedures are used, and for a quadratic interpolation scheme. The initial term structure is given by:

$$f(0,t) = 0.07 - 0.02e^{-0.18t}.$$

The case parameters for the volatility structure are:

$$\kappa = 0.1,\ a_0 = 0.02,\ a_1 = 0.0025,\ b_0 = 0.003.$$

In this case there are three state variables in the model.

**Table 3**
**Weekly Estimates of Parameters***

| | GV Estimates | | GGV Estimates | | | | | |
|---|---|---|---|---|---|---|---|---|
| week | $a_0$ | k | $a_0$ | $a_1$ | $b_0$ | k | Hump | Max. Vol. |
| 1 | 0.0133 | 0.0346 | -0.0221 | 0.0410 | 0.0100 | 1.3087 | 1.3034 | 0.0157 |
| 2 | 0.0129 | 0.0282 | -0.0203 | 0.0363 | 0.0101 | 1.2647 | 1.3497 | 0.0153 |
| 3 | 0.0130 | 0.0263 | -0.0230 | 0.0401 | 0.0104 | 1.3394 | 1.3193 | 0.0155 |
| 4 | 0.0131 | 0.0239 | -0.0230 | 0.0400 | 0.0107 | 1.3679 | 1.3054 | 0.0156 |
| 5 | 0.0131 | 0.0226 | -0.0328 | 0.0535 | 0.0109 | 1.5416 | 1.2627 | 0.0158 |
| 6 | 0.0131 | 0.0201 | -0.0308 | 0.0506 | 0.0111 | 1.5326 | 1.2612 | 0.0158 |
| 7 | 0.0132 | 0.0259 | -0.0273 | 0.0470 | 0.0107 | 1.4548 | 1.2683 | 0.0158 |
| 8 | 0.0130 | 0.0265 | -0.0271 | 0.0468 | 0.0105 | 1.4697 | 1.2579 | 0.0156 |
| 9 | 0.0130 | 0.0226 | -0.0232 | 0.0387 | 0.0105 | 1.3007 | 1.3695 | 0.0155 |
| 10 | 0.0131 | 0.0231 | -0.0216 | 0.0373 | 0.0106 | 1.3095 | 1.3439 | 0.0155 |

* Table 3 shows the implied estimates of the forward rate volatility parameters in each of 10 successive weeks. Each estimate is based on 45 caplet prices spanning the maturity spectrum.

**Table 4**
**In-Sample Residual Analysis +**

| Model | Caplet Maturity | 1 | 2 | 3 | 4 | 5 | 6 | 7 | 8 | 9 |
|---|---|---|---|---|---|---|---|---|---|---|
| GV | positive | 0* | 50* | 50* | 50* | 48* | 17 | 3* | 2* | 14* |
| | negative | 50 | 0 | 0 | 0 | 2 | 33 | 47 | 48 | 36 |
| | average | -3.330* | 0.763* | 0.684* | 0.455* | 0.269* | -0.087* | -0.178* | -0.206* | -0.094* |
| | s.d. | 0.290 | 0.165 | 0.164 | 0.155 | 0.150 | 0.200 | 0.132 | 0.140 | 0.141 |
| GGV | positive | 23 | 37* | 9* | 32 | 42* | 21 | 22 | 19 | 32 |
| | negative | 27 | 13 | 41 | 18 | 8 | 29 | 28 | 31 | 18 |
| | average | -0.007 | 0.055* | -0.124* | 0.021 | 0.137* | -0.038 | -0.041* | -0.046* | 0.043* |
| | s.d. | 0.177 | 0.170 | 0.170 | 0.150 | 0.144 | 0.194 | 0.132 | 0.135 | 0.134 |

+ Table 4 shows the in-sample residuals by caplet maturity. For example, the GV model produce 48 positive residuals and two negative residuals for the 5 year maturity caplet. The starred values indicate the proportions (means) that were significantly different from one half (zero). All test were done at 0.5% level of significance.

**Table 5**
**Out-of-Sample Residual Analysis +**

| Model | Maturity | 1 | 2 | 3 | 4 | 5 | 6 | 7 | 8 | 9 |
|---|---|---|---|---|---|---|---|---|---|---|
| GV | positive | 0* | 44* | 44* | 43* | 38* | 24 | 14* | 17 | 24 |
| | negative | 45 | 1 | 1 | 2 | 7 | 21 | 31 | 28 | 21 |
| | average | -3.363* | 0.760* | 0.700* | 0.480* | 0.298* | -0.044 | -0.130* | -0.138* | -0.030 |
| | s.d. | 0.347 | 0.247 | 0.250 | 0.242 | 0.244 | 0.304 | 0.236 | 0.239 | 0.246 |
| GGV | positive | 25 | 26 | 16 | 30 | 35* | 26 | 26 | 27 | 30 |
| | negative | 20 | 19 | 29 | 15 | 10 | 19 | 19 | 18 | 15 |
| | average | -0.037 | 0.038 | -0.111* | 0.048 | 0.168* | 0.007 | 0.008 | 0.017 | 0.101* |
| | s.d. | 0.406 | 0.275 | 0.247 | 0.227 | 0.231 | 0.301 | 0.234 | 0.239 | 0.252 |
| GV Wins** | | 0 | 3 | 6 | 6 | 9 | 23 | 20 | 21 | 27 |
| GGV Wins | | 45* | 42* | 39* | 39* | 36* | 22 | 25 | 24 | 18 |
| Number of Trials | | 45 | 45 | 45 | 45 | 45 | 45 | 45 | 45 | 45 |

+ Table 5 shows the out-of-sample residuals by caplet maturity. For example, the GV model produces 38 positive residuals and 7 negative residuals for the 5 year caplet. The starred values indicate the proportions (means) that were significantly different from one half (zero). All test were done at 0.5% level of significance.

** GV wins if the absolute value of the residual is smaller than the absolute value of the corresponding GGV model. Otherwise GGV wins.

Table 6
Analysis of GGV Residuals Over Out-of-Sample Periods*

| Residuals | day 1 | day 2 | day 3 | day 4 | day 5 |
|---|---|---|---|---|---|
| \|0.00\| - \|0.25\| | 68 | 52 | 46 | 43 | 43 |
| \|0.25\| - \|0.50\| | 11 | 26 | 31 | 30 | 28 |
| \|0.50\| - \|0.75\| | 2 | 2 | 3 | 8 | 7 |
| > \|0.75\| | 0 | 1 | 1 | 0 | 3 |

* This table provides the distribution of the residuals for each day in the out-of-sample periods. For example, of the 81 residuals in the last day of the out-of-sample period, 43 were within 0.25 vols of the actual price.